Royal Norwegian Council
for Scientific and Industrial Research
(NTNF)

NORSAR

NORSAR Scientific Report No. 2-89/90

Semiannual Technical Summary

1October 1989 — 31 March 1990

Kjeller, June 1990

APPROVED FOR PUBLIC RELEASE, DISTRIBUTION UNLIMITED

7.4 Ray-based interpretation of Lg azimuth anomalies at NORESS

Introduction

In a recent paper, Bostock and Kennett (1990) introduced a method for predicting the propagation characteristics of the Lg phase in areas of complex crustal structure in a semiquantitative manner. The method relies on the interpretation of Lg as constructively interfering S waves multiply reflected within the earth's crust. A set of rays is traced outwards from a point source within a crustal waveguide of variable thickness. The geometrical characteristics of the rays are modified upon reflection from the crust-mantle boundary and the free surface according to Snell's law, and can then be monitored in plan view by the horizontal projection of the rays and the location of mantle reflection points. This approach allows a qualitative description of a variety of complex propagation processes including mode coupling, wavetype conversion, and lateral waveguiding for situations which, because of difficulties in handling boundary conditions, cannot be adequately described by current quantitative, modal descriptions of the Lg phase (see, e.g., Kennett, 1989). More specifically, it is possible to associate changes in the separation of S-wave reflection points with a change in the character of the wavefield viewed as a sum of higher mode surface waves since the angle a ray makes with the vertical may be related to an equivalent phase velocity. In addition, the polarization of the S waves may be used as a measure of the conversion between Love and Rayleigh waves.

Although the method has been used to explain the observed patterns of Lg propagation in central Asia (Bostock and Kennett, 1990) and the southwestern United States (Kennett *et al*, 1990), its success is highly dependent upon the knowledge of crustal model. In these previous studies, variation in crustal thickness was considered the dominant factor influencing the character of Lg on seismograms, and crustal models based on varying degrees of isostatic compensation were adopted in accordance with published geophysical and tectonic evidence. However, there are a number of other factors which may become significant in general applications. For instance, in areas of thick sedimentary cover it may be advisable to consider that portion of the crust comprising basement alone. In general, the effects of vertical velocity structure and systematic lateral variations therein will generally be insignificant at all but the lowest phase velocities, however abrupt lateral heterogeneity in physical properties will undoubtedly play an important role in distorting the observed wavefield. A truly quantitative representation of Lg propagation using the ray method is only possible when comprehensive information on all contributing factors is incorporated in the construction of our crustal models. Notwithstanding, in many cases valuable insight may be gained by considering simply the variation in crustal thickness, in which case an accurate knowledge

of the depth to Moho is essential since fluctuations in this lower boundary are, in general, more pronounced than those at the free surface.

Scandinavia crustal model

Our objective in this study is to employ the ray method as a tool in assessing the effects of gross crustal structure on Lg propagation in Scandinavia and adjacent areas to the east, and relating the predicted behavior to azimuth anomalies observed at the small-aperture NORESS array. We will therefore consider a single-layer crustal model over the area 0°–35°E, 55°–75°N comprising all of Scandinavia and Finland and parts of the Soviet Baltic states. The modelled free surface boundary is a smoothed (81 point average) version of relief data from the ETOPO5 world topography data base at 5' intervals. The crust-mantle boundary was constructed by interpolating the Moho map of Ruud (pers. comm.) which combines information from a variety of geophysical studies (seismic reflection, refraction, gravity, etc.) and is thought to be an accurate representation of the main low-wavelength structure over the region. The main topographic feature is the Caledonide Range paralleling the coast of Norway, which rises to an elevation of 2000+ m over a considerable area. The Moho map shown in Fig. 7.4.1 presents a slightly more complicated picture. The mean sea level depth to Moho decreases rapidly off the Norwegian coast to typical values for oceanic crust ($\sim$ 10 km). Interestingly, the Caledonides are not mirrored by any significant root on the Moho; rather, crustal thicknesses generally increase steadily as one approaches the center of the Baltic Shield. There are several areas of increased crustal thickness ($>$ 50 km); notably along the central and northern portions of the Soviet-Finnish border, and a saddle-shaped structure straddling the eastern coast of Sweden. Moho depths tend to decrease further south and east approaching the Russian platform.

Ray analysis

Mykkeltveit *et al* (1989) have assembled a data base of Lg azimuth anomalies observed at NORESS from a variety of sources at distances from 100 to 1000 km which indicates that in some regions there is extreme variability in the magnitude and sign of azimuth anomalies with even minor changes in source position. We will examine possible causes for this anomaly distribution using the ray technique discussed above.

Perhaps the most interesting region in terms of anomalous behavior is located along the southern coast of Finland on the Gulf of Bothnia. Here Lg waves from sources separated by distances as small as 2°–3° in latitude exhibit strikingly different azimuthal anomalies. To investigate this behavior, we present ray diagrams generated for i) different phase velocities at a single

source location (21°E, 60°N) in Fig. 7.4.2, and ii) different source locations in this general area (21°E, 59.0°–62.0°N) at constant phase velocity (4.0 km/s) in Fig. 7.4.3.

We first describe the variable phase velocity diagrams shown in Fig. 7.4.2. For lower phase velocities (e.g., 3.8 km/s — Fig. 7.4.2a) guided wave propagation is generally less affected by lateral variation in crustal thickness as an individual ray undergoes fewer bounces over a given distance. The figure also indicates that a large proportion of the rays undergo reflection at the continental margin off western Norway accompanied by conversion to Sn mantle phases into the oceanic crust (denoted by solid diamonds). Of specific relevance is the saddle-shaped low in Moho relief centered roughly midway between NORESS and the source, and occupying a significant portion of the total path (see also Fig. 7.4.1). Note that the axis of the ridge separating the two pockets is roughly colinear with a line joining NORESS and the source. We recall that zones of increased crustal thickness tend to behave as attractors, pulling rays inward in much the same fashion as high velocity zones in conventional body wave raytracing. Hence as a general observation, rays launched at all 3 phase velocities tend to be drawn away from the Moho ridge leaving windows through which fewer rays pass. These windows overlap for the three ray diagrams (Figs. 7.4.2a, b, c) but do not exactly coincide since the phase velocity dictates the exact location of the basement reflection points for a given ray and their resulting ray curvature. The position of NORESS relative to these alternate low and high ray density windows is therefore a function of phase velocity, and we might accordingly expect the azimuth of the observed wavetrain to vary considerably with time as the individual phase velocity components arrive at different group velocities. In addition, observed azimuths are likely to depend significantly on the frequency characteristics of the particular source-excitation function.

We now consider the effect of shifting the source by 1° increments along the 21° E meridian on ray diagrams generated at a fixed phase velocity of 4.0 km/s as shown in Fig. 7.4.3. Note that even small changes in source position can significantly alter the source-heterogeneity-receiver geometry. The ray diagrams reflect this fact by exhibiting considerable variation in ray density west of the main heterogeneity: the saddle-shaped low in Moho relief behaves as a lens which focuses and defocuses ray bundles in a way that is strongly dependent on the location of the illuminating source.

Finally we examine a more distant source at the head of the Gulf of Estonia. The ray diagram in Fig. 7.4.4 indicates that the absence of major heterogeniety along the initial part of the ray paths results in a ray pattern which remains quite coherent into eastern Sweden. Rays in the vicinity of the heterogeneity are more nearly parallel than those from closer sources (as in Figs. 7.4.2 and 7.4.3) and tend not to diverge as markedly upon transmission. Nevertheless,

the effects of the Moho saddle are still manifest in a focusing and defocusing of rays which, for the particular phase velocity employed, leaves NORESS in a region of low ray density.

Discussion

Initial attempts to relate ray-calculated and observed azimuth anomalies yielded somewhat inconsistent results, but upon careful examination of the ray behavior it becomes evident that the nature of the Moho heterogeneity in the vicinity of NORESS is probably largely responsible. In areas of broader scale heterogeneity, ray diagrams are characterized by more systematic and gradual changes in ray pattern with respect to both source location and phase velocity (see for example Bostock and Kennett, 1990). The complexity of the Moho saddle east of NORESS, its comparatively complicated geometry over a region of restricted spatial extent, results however in ray diagrams which are considerably more sensitive to these two parameters. The observations made above would appear to bear important implications to the analysis of crust and upper mantle phases originating from parts east of the array, especially for more proximal sources. The study suggests that the Moho saddle, a feature which appears to be well defined and documented in a number of independent investigations, will play a significant role in distorting the wavefield and is probably responsible in large part for the Lg azimuth anomalies observed at NORESS from sources to the east.

M.G. Bostock & B.L.N. Kennett, Research School of Earth Sciences
Australian National University, Canberra
S. Mykkeltveit, NORSAR

References

Bostock, M.G. and B.L.N. Kennett (1990): Lg propagation patterns in three dimensional heterogeneity, *Geophys. J. Intl.*, in press.

Kennett, B.L.N. (1989): Lg waves in heterogeneous media, *Bull. Seism. Soc. Am.*, **79**, 860–872.

Kennett, B.L.N., M.G. Bostock and J.-K. Xie (1990): Guided-wave tracking in 3-D — a tool for interpreting complex regional seismograms, *Bull. Seism. Soc. Am.*, in press.

Mykkeltveit, S., S. Kibsgaard and T. Kværna (1989): Region-specific knowledge derived from analysis of NORESS data, in *NORSAR Basic Seismological Research, 1 January - 30 September 1989, Annual Technical Report, Contract No. F49620-89-C-0038*, ed. S. Mykkeltveit.

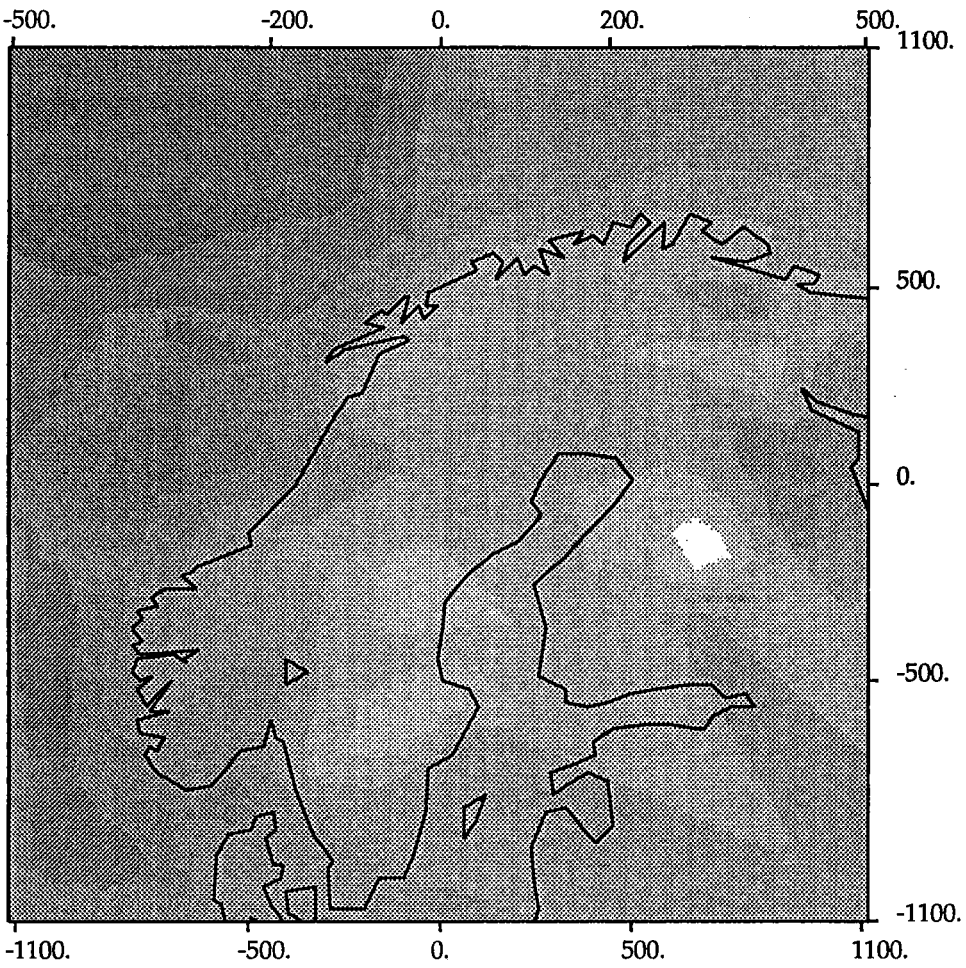

SCALES

Horizontal - km as marked

Vertical - km below msl

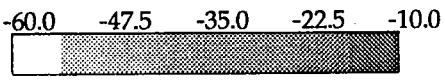

Fig. 7.4.1. Moho relief over Scandinavia, Finland and the Soviet Baltic states after Ruud (pers. comm.); lighter shades indicate increased Moho depths. The location of the NORESS array is marked by a triangle.

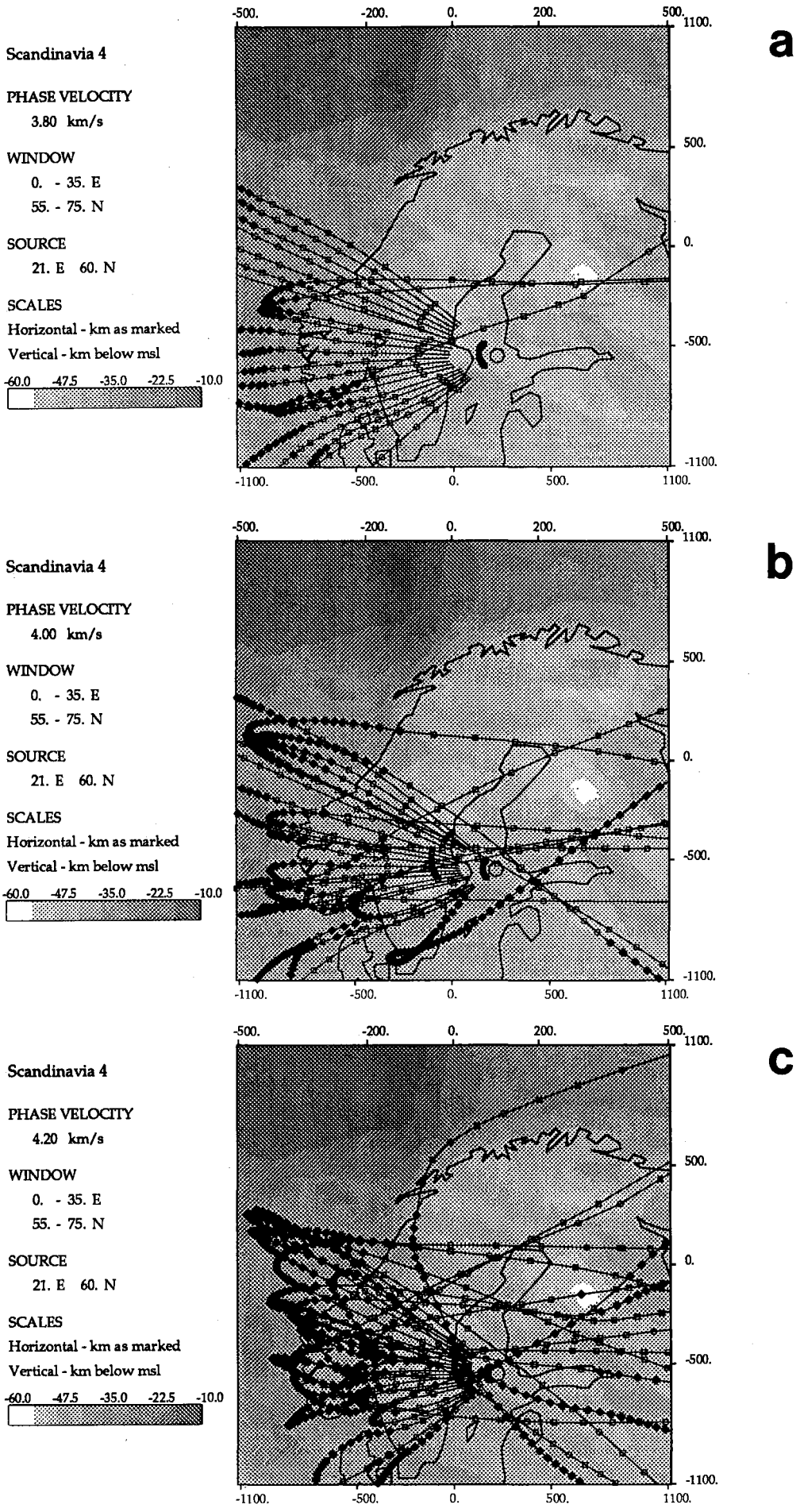

Fig. 7.4.2. Ray diagrams for a source located at 21°E, 60°N at three phase velocities a) 3.8 km/s, b) 4.0 km/s and c) 4.2 km/s. Note alternating high and low ray-density windows resulting from Moho saddle east of NORESS.

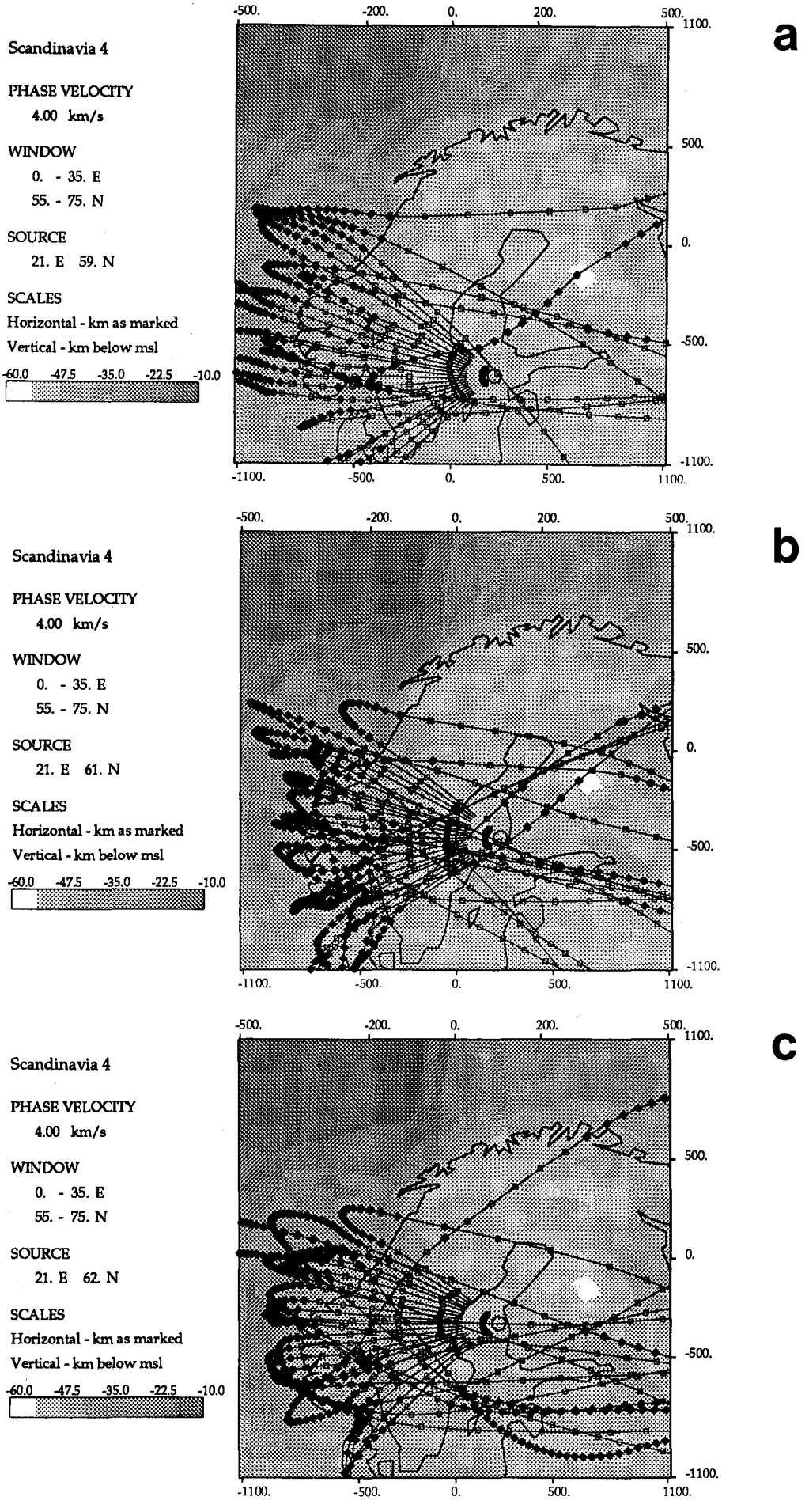

Fig. 7.4.3. Ray diagrams for 3 sources located at a) 21°E, 59°N, b) 21°E, 61°N and c) 21°E, 62°N at a phase velocity of 4.0 km/s. Note variability of ray patterns with source location.

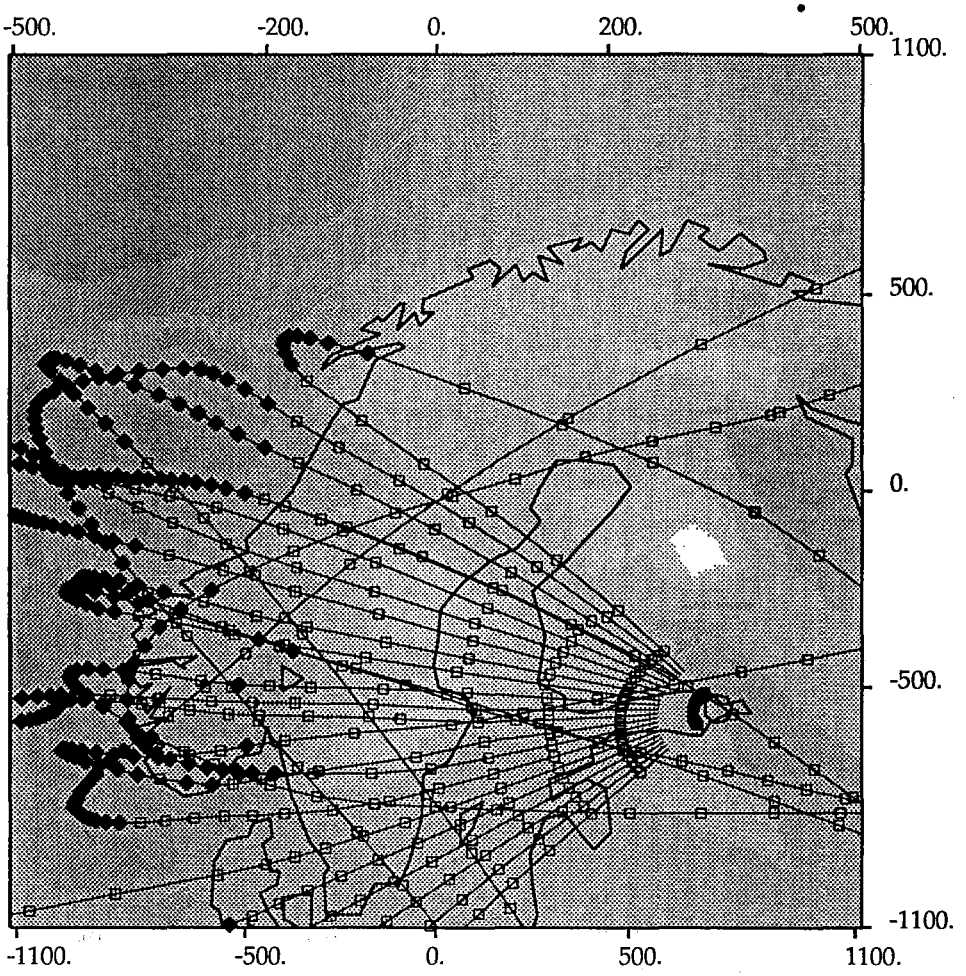

Gulf of Estonia 2

PHASE VELOCITY

4.00 km/s

WINDOW

0. - 35. E

55. - 75. N

SOURCE

29. E 60. N

SCALES

Horizontal - km as marked

Vertical - km below msl

-60.0 -47.5 -35.0 -22.5 -10.0

Fig. 7.4.4. Ray diagram for a source in the eastern Gulf of Estonia at a phase velocity of 4.0 km/s. Note the relative coherence in the ray pattern east of the Swedish coast.